

Supporting Information

Study on the Attachment of *Escherichia coli* to Sediment Particles at a Single-Cell Level: the Effect of Particle Size

Tao Wu¹, Chunhui Zhai^{2,†}, Jingchao Zhang^{2,†}, Dejun Zhu^{1,*}, Kun Zhao^{2,*} and Yongcan Chen^{1,3}

¹ State Key Laboratory of Hydrosience and Engineering, Tsinghua University, Beijing 100084, China; wutao15@mails.tsinghua.edu.cn (T.W.); chenyc@tsinghua.edu.cn (Y.C.)

² Key Laboratory of Systems Bioengineering (Ministry of Education), School of Chemical Engineering & Technology, Tianjin University, Tianjin 300072, China; chunhuizhai@tju.edu.cn (C.Z.); 2015207553@tju.edu.cn (J.Z.)

³ Southwest University of Science and Technology, 59 Qinglong Road, Mianyang 621010, Sichuan, China

[†] These authors contributed equally to this work

^{*} Correspondence: kunzhao@tju.edu.cn (K.Z.); zhudejun@tsinghua.edu.cn (D.Z.); Tel.: +86-135-0361-1666 (K.Z.); +86-10-62772255 (D.Z.)

1. *E. coli* Concentration Validation through Estimation of *E. coli* Flux in Microfluidic Devices

In the flow cells we choose observation fields at different positions, and the dimensions of each observation field were $67.5 \mu\text{m} \times 67.5 \mu\text{m} \times 20\text{--}30 \mu\text{m}$. Videos of the observation fields were recorded using the microscope and camera, and then the number of *E. coli* passed through was counted and the flux at the positions was calculated according to Equation (1).

$$\Phi_p(t) = \frac{N_{count}(t)}{tb_{vf}h_{vf}} \quad (1)$$

where N_{count} = the total number of bacteria passing through the boundary for time duration t ; l_{vf} = the width of the observation field, μm ; h_{vf} = the thickness of the counting area, μm .

Due to the limited depth of focus of the microscope, z-scan was performed in a loop manner during the video recording. In order to improve the statistics of results, a rectangular block region was chosen to record the bacterial passage through a big volume. Thus the height of the rectangular block should be chosen to be as large as possible to include more volume under the constraint that there is no cell missed during the bottom-to-top scan period. In other words, the bottom-to-top scan should be quick enough so that during one bottom-to-top scan, the moving distance of a cell would not exceed the length of the rectangular block region along the flow direction. In the experiments, each recording lasted for 15 minutes. The length and width of the rectangular block for observation are both $67.5 \mu\text{m}$, and the height is $20 \mu\text{m}$ to $30 \mu\text{m}$. The step size of z-scan was set to $0.9 \mu\text{m}$ at minimum. It took 7.5 s to finish one bottom-to-top scan for a block with $30 \mu\text{m}$ height and 4.7 s for a block with $20 \mu\text{m}$ height. Under this set-up, no cell would be missed during a z-scan, and the number of *E. coli* can be counted accurately.

E. coli fluxes at different positions (Figure S1a) were measured as described above. Among the selected positions, L_a , L_b and L_c have the same x and y coordinates but different z coordinates (z_a : $0\text{--}20 \mu\text{m}$; z_b : $20\text{--}50 \mu\text{m}$ and z_c : $100\text{--}130 \mu\text{m}$). L_b , L_d and L_e have the same x and z coordinates but different y coordinates (y_a : $0 \mu\text{m}$; y_b : $1000 \mu\text{m}$; y_c : $2000 \mu\text{m}$). L_e is near the side wall of the channel.

L_a and L_b are typical locations where particles are picked for attachment measurements. All other positions are only for the purpose of uniformity assessment of bacterial flux.

The obtained curves exhibited fluctuation at early stage due to small sample numbers but approached to a constant at long times given enough statistical events. Figure S1b showed that all curves approached to a constant starting at about 900 s . Then the cumulative average value at 900 s was used as the average *E. coli* flux Φ_p at the corresponding position.

The measured *E. coli* fluxes showed variations at different positions. At L_e that is close to the side wall, the *E. coli* flux is the highest. This result may be induced by ‘shear-trapping’. Some motile cells like *E. coli* tend to be depleted in low shear region and accumulate in high shear region, owing to the alignment of swimming direction with fluid streamlines caused by shear forces [1].

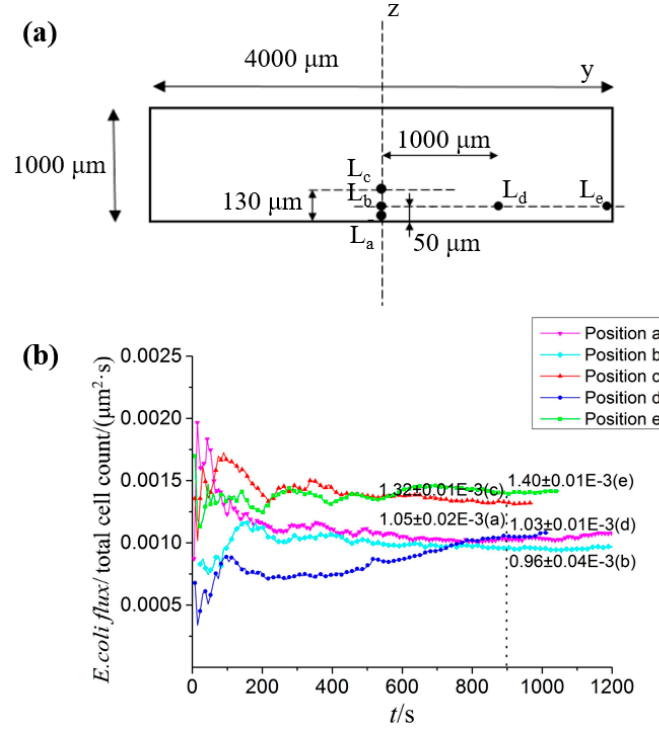


Figure S1. *E. coli* flux measurement and results. (a) Picked positions for measuring *E. coli* flux in the cross-section of the channel. (b) The cumulative average of *E. coli* flux at selected positions.

The average *E. coli* flux of the entire flow-cell $\bar{\Phi}$ could be calculated as the mean value of bacterial fluxes at selected locations, Φ_a , Φ_b , Φ_c , Φ_d and Φ_e . Then the average bacterial concentration C_w (at OD = 0.01) can be obtained from Equation (2):

$$\bar{\Phi} = \frac{QC_w}{S_{channel}} \quad (2)$$

where Q = the flow rate, mL/s; $S_{channel}$ = the cross-section area of the channel, μm^2 . The calculated C_w was 5.54×10^9 total cell count/L. On the other hand, the concentration of the *E. coli* suspension was also measured using the membrane filtration method. And the measured result was 5.4×10^9 cfu/L. The concentrations measured by two different methods agreed. So *E. coli* die-off in our microfluidic experiments was negligible, which meant that total cell count in the micro level can be considered numerically equivalent to colony forming units in the macro level.

2. Surface Morphology of Particles

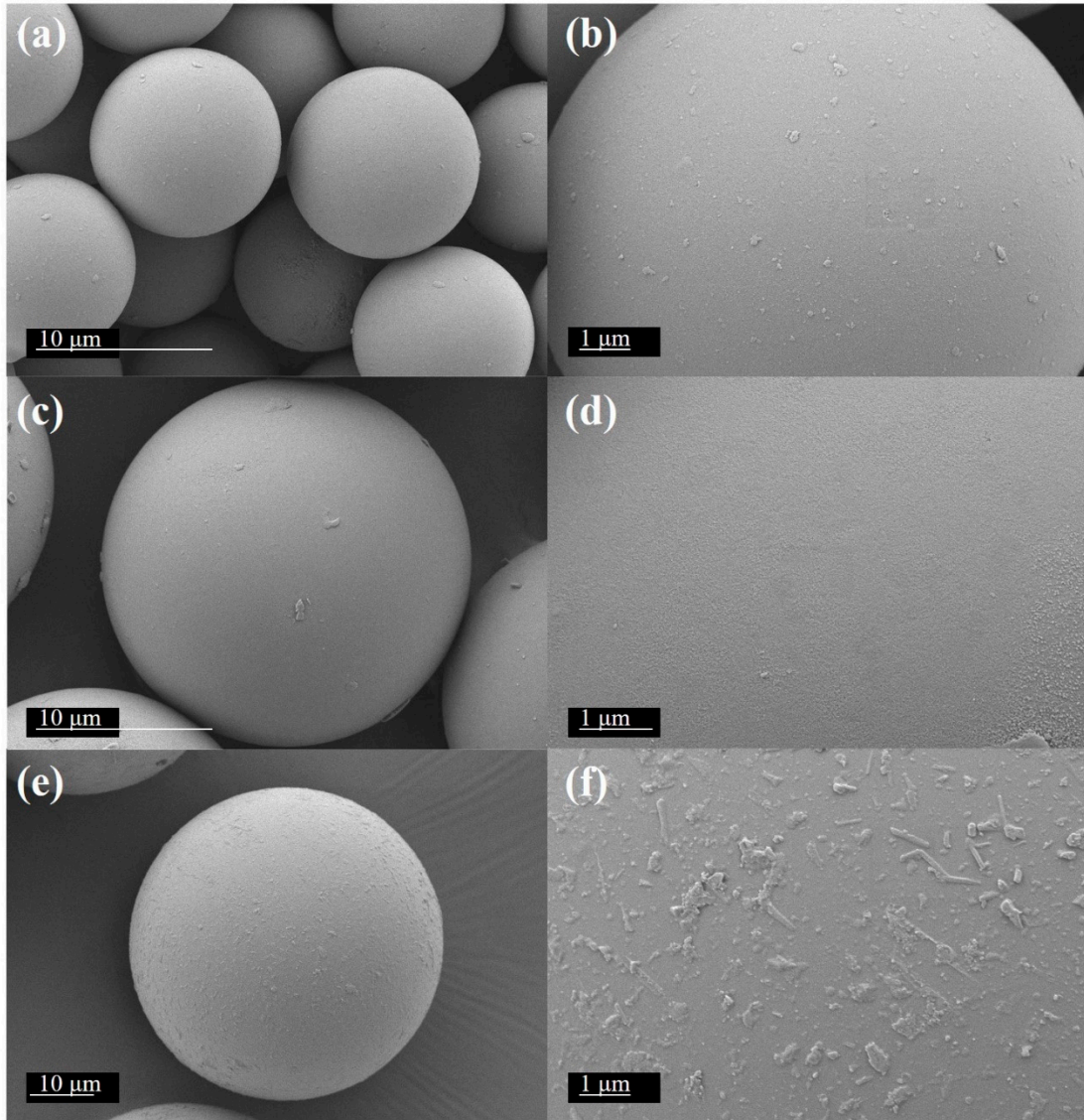


Figure S2. SEM micrographs of glass microspheres. (a) 10 µm microspheres at low magnification ($\times 10k$); (b) 10 µm microspheres at high magnification ($\times 30k$); (c) 20 µm microspheres at low magnification ($\times 10k$); (d) 20 µm microspheres at high magnification ($\times 30k$); (e) 50 µm microspheres at low magnification ($\times 3.6k$); (f) 50 µm microspheres at high magnification ($\times 20k$).

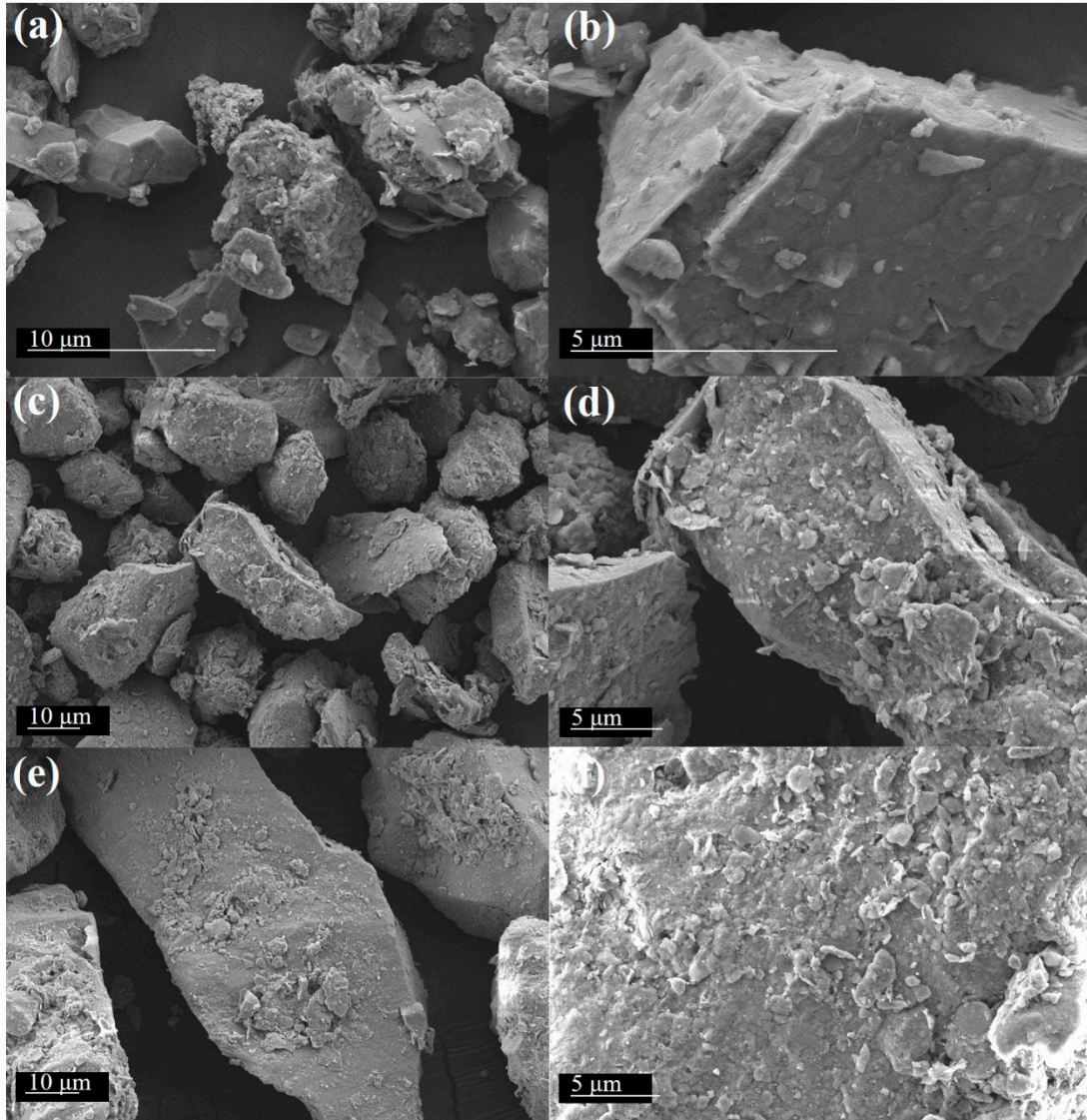


Figure S3. SEM micrographs of sediment particles. (a) 10 μm sediment particles at low magnification ($\times 10\text{k}$); (b) 10 μm sediment particles at high magnification ($\times 30\text{k}$); (c) 20 μm sediment particles at low magnification ($\times 3\text{k}$); (d) 20 μm sediment particles at high magnification ($\times 10\text{k}$); (e) 50 μm sediment particles at low magnification ($\times 3\text{k}$); (f) 50 μm sediment particles at high magnification ($\times 10\text{k}$).

References

1. Barry, M.T.; Rusconi, R.; Guasto, J.S.; Stocker, R. Shear-induced orientational dynamics and spatial heterogeneity in suspensions of motile phytoplankton. *J. R. Soc. Interface* **2015**, *12*.